Hardcastle and R. Mason for communicating their results prior to publication, and Ms. E. Boespflug for preparation of some of the complexes.

Registry No. $[CpFeCO]_2Ph_2P(CH_2)PPh_2$, 60508-02-3; $\{[CpFeCO]_2Ph_2P(CH_2)PPh_2\}BPh_4$, 12701-56-3; $[CpFeCO]_2Ph_2P(CH_2)_2PPh_2$, 12701-59-6; $\{[CpFeCO]_2Ph_2P(CH_2)_2PPh_2\}BPh_4$, 12701-60-9.

References and Notes

(1) (a) R. J. Haines and A. L. du Preez, *J. Organomet. Chem.*, **21**, 181 (1970); (b) R. J. Haines and A. L. du Preez, *Inorg. Chem.*, **11**, 330 (1972).
(2) T. J. Meyer, *Prog. Inorg. Chem.*, **19**, 1 (1975).
(3) M. B. Robin and P. Day, *Adv. Inorg. Radiochem. Chem.*, **10**, 248 (1967).
(4) N. S. Hush, *Chem. Phys.*, **10**, 361 (1975).
(5) T. Åberg, *Phys. Rev.*, **156**, 35 (1969); *Ann. Acad. Sci. Fenn., Ser. A6*, **308**, 1 (1969).
(6) J. A. Ferguson and T. J. Meyer, *Inorg. Chem.*, **11**, 631 (1972).
(7) K. Hardcastle and R. Mason, private communication.
(8) B. F. Hallam and P. L. Pauson, *J. Chem. Soc. A*, 3030 (1956).
(9) R. F. Fenske and M. B. Hall, *Inorg. Chem.*, **11**, 768 (1972).
(10) O. S. Mills, *Acta Crystallogr.*, **11**, 620 (1958).
(11) F. A. Cotton and J. M. Troup, *J. Am. Chem. Soc.*, **96**, 4422 (1974).
(12) J. W. Richardson, W. C. Nieuwpoort, R. R. Powell, and W. F. Edgell, *J. Chem. Phys.*, **36**, 1057 (1962).
(13) M. Barber, J. A. Connor, M. F. Guest, M. B. Hall, I. H. Hillier, and W. N. E. Meredith, *Faraday Discuss. Chem. Soc.*, **54**, 219 (1972).
(14) "Tables of Atomic Functions", a supplement to a paper by E. Clementi, *IBM J. Res. Dev.*, **9**, 2 (1965).
(15) D. D. Radtke, Ph.D. Thesis, University of Wisconsin, 1966.
(16) L. J. Aarons, M. Barber, M. F. Guest, I. H. Hillier, and J. H. McCartney, *Mol. Phys.*, **26**, 1247 (1973).
(17) L. J. Aarons, M. F. Guest, M. B. Hall, and I. H. Hillier, *J. Chem. Soc., Faraday Trans.*, 563 (1973).
(18) W. L. Jolly and D. N. Hendrickson, *J. Am. Chem. Soc.*, **92**, 1863 (1970); J. M. Hollander and W. L. Jolly, *Acc. Chem. Res.*, **3**, 193 (1970).
(19) A reviewer has suggested that one should not identify the two orbitals of Hush's model with particular orbitals of a full MO calculation but rather with the average value of the manifold of bonding and antibonding orbitals, respectively. The main metal–metal bonding orbitals are $13b_1$, $18a_1$, and $17a_1$, and the main metal–metal antibonding orbitals are $15b_2$, $8a_2$, and $14b_2$. Averaging these groups of orbitals, we obtained $2J = 2.71$ eV. Applying a similar averaging to the core-hole state, we obtained $\Delta = 5.57$ eV. The satellite is then predicted to be 40% of the main peak.

Contribution from the Department of Chemistry, University of Missouri—Rolla, Rolla, Missouri 65401

Mössbauer, Electronic, and Structural Properties of Several Bis- and Tetrakis(pyridine)iron(II) Complexes

BILL F. LITTLE and GARY J. LONG*

Received December 7, 1977

The high-spin tetrakis(pyridine)iron(II) complexes $Fe(py)_4X_2$, where X is Cl, Br, I, NCO, NCS, and NCSe, have a tetragonally distorted trans octahedral structure. Magnetically perturbed Mössbauer spectra for each of these compounds indicate a positive electric field gradient tensor and a nondegenerate orbital ground term. An angular overlap analysis of the quadrupole interaction in these compounds indicates that, relative to chlorine and bromine and the pseudohalides, pyridine is a poor π-bonding ligand and is comparable to iodine. The high-spin pseudooctahedral $Fe(py)_2X_2$ complexes, where X is Cl, Br, NCO, NCS, and NCSe, have polymeric linear-chain structures with bridging anions and trans pyridine ligands. The thiocyanate and selenocyanate complexes have both nitrogen and sulfur or selenium coordinated to adjacent iron atoms whereas the cyanate anion bridges via a three-center bond at the nitrogen atom. The Mössbauer spectra of the bis(pyridine) chloride, thiocyanate, and selenocyanate complexes reveal spontaneously ordered one-dimensional ferromagnets at 4.2 and 1.3 K. The Mössbauer spectrum at 4.2 and 1.1 K reveals that $Fe(py)_2Br_2$ is paramagnetic. No spontaneous ordering is observed at 4.2 K in a 6-T applied field. The electronic spectra at room temperature and at 23 K for all of these complexes have been evaluated in terms of the angular overlap model. The results indicate that pyridine is a better σ-bonding ligand than the halide or pseudohalide ligands. In general, the monodentate nonbridging halides and pseudohalides are better σ-bonding ligands than are the bridging ligands. The infrared and powder X-ray diffraction results—which indicate many isomorphisms with the analogous cobalt and nickel complexes—are consistent with the above structural assignments. All evidence indicates that $Fe(py)_2I_2$ has a pseudotetrahedral structure.

Introduction

The bis- and tetrakis(pyridine) complexes of iron(II) halides and pseudohalides provide a means to study the structural, magnetic, and electronic properties of a compound as a function of the iron–ligand bond. This paper, a continuation of our earlier work on $Fe(py)_2Cl_2$[1] and $Fe(py)_2(NCS)_2$,[2] reports an investigation of the chloro, bromo, iodo, cyanato, thiocyanato, and selenocyanato complexes with pyridine. The incentive for this further work results from the structural isomers possible for the bis complexes, the existence of a metamagnetic transition,[3,4] and a structural phase transition[5] in certain of these complexes, as well as their suitability for study by optical and Mössbauer spectral techniques. Although there have been many earlier Mössbauer effect,[6-15] magnetic,[6,8,16-18] infrared,[19] optical,[8,20,21] and thermal[10,11,14,15] studies of individual iron–pyridine complexes, this work represents the first unified study of the bonding in these complexes for a series of anions.

Experimental Section

All operations were carried out in a Vacuum Atmospheres Inc. inert-atmosphere glovebox filled with nitrogen. Solid reagent grade chemicals were used without further purification. All solvents were dried and deoxygenated by standard laboratory procedures. Spectroscopic grade pyridine was either distilled under a steam of dry nitrogen or stored over a molecular sieve. Elemental analyses for all compounds are reported in Table I.[22]

Preparation of Tetrakis(pyridine)iron(II) Complexes. These complexes were prepared by modifications of previously reported procedures.[1,6,16,21,23] These compounds are stable for many months when stored in an inert atmosphere in the dark. More synthetic details are available elsewhere.[24]

Preparation of Bis(pyridine)iron(II) Complexes. $Fe(py)_2Cl_2$ was prepared directly according to method A described previously by Long et al.[1]

In the preparation of $Fe(py)_2Br_2$, 0.022 mol of bromine, dissolved in 25 mL of deoxygenated methanol, was slowly added to an excess of reduced iron powder, stirred for several hours, and filtered twice to remove all traces of iron. To this solution 0.045 mol of freshly distilled pyridine was slowly added with stirring. A yellow crystalline precipitate formed within several minutes and was filtered, washed with a 50% by volume solution of anhydrous methanol and diethyl ether, and dried for 1 h under a static vacuum.

$Fe(py)_2I_2$ was prepared by heating $Fe(py)_4I_2$ under vacuum at 82 °C for 8 h in an Abderhalden drying apparatus. During this heating, the bright yellow crystals of the tetrakis complex underwent a 25.28% weight loss, a 50.0% pyridine loss, and became light yellow.

$Fe(py)_2(NCO)_2$ was prepared from $Fe(py)_4(NCO)_2$ by two different thermolytic procedures. In the first, hydrogen gas (purified by passage over copper turnings and iron wool at 550 °C and then through a liquid nitrogen trap) was passed over $Fe(py)_4(NCO)_2$ in a reduction tube held at 88 °C for 16 h. The weight loss of 34.6% corresponded to

0020-1669/78/1317-3401$01.00/0

a loss of 49.9% pyridine. The yellow tetrakis complex changed to pale yellow during thermolysis. In the second, preferable, procedure, the thermolysis was carried out by heating $Fe(py)_4(NCO)_2$ in a vacuum of ca. 10^{-3} torr at 55 °C for 19 h. The weight loss of 34.16% corresponded to a loss of 49.3% pyridine and the same color change occurred. Special care is necessary to prevent exposure of the product to oxygen and water. The temperature of thermolysis must be carefully controlled at 55 °C. Above 62 °C, excess pyridine is lost. Below 55 °C, the required loss of pyridine becomes excessively time consuming. Carbon, hydrogen, and nitrogen analyses for this compound are not reported in Table I[22] because an apparent decomposition in transit or during analysis at the microanalytical laboratory resulted in random and meaningless results. The value for iron given in Table I[22] is the average of four values obtained on four different preparations. A spectrophotometric analysis in absolute methanol found 52.6% by weight of pyridine in two different samples. $Fe(py)_2(NCO)_2$ is 53.1% by weight pyridine.

$Fe(py)_2(NCS)_2$ was prepared by thermolysis of $Fe(py)_4(NCS)_2$ under a stream of pure hydrogen (obtained as described above) for 8 h at 140 °C. The sample lost 32.46% of its weight and 50.1% of its pyridine, and the product is light yellow. The purified hydrogen prevented the formation of trace amounts of an iron(III) thiocyanate species[25] which absorbs at ca. 20 000 cm^{-1}.

$Fe(py)_2(NCSe)_2$ was prepared by the thermolysis of $Fe(py)_4(NCSe)_2$ under a stream of pure hydrogen (obtained as described above) for 10 h at 140 °C. The sample lost 26.84% of its weight and 49.4% of its pyridine, and the product is light yellow. When a small sample of $Fe(py)_2(NCSe)_2$ was exposed to the atmosphere, its color changed to a rust red within 10 min.

The cobalt and nickel complexes, used primarily for X-ray comparative studies, were prepared by standard methods such as those presented in ref 26 and elsewhere.[27-34] More details are presented elsewhere.[24]

Physical Measurements. Electronic absorption spectra were recorded on a Cary 14 in Fluorolube GR-90 grease mulls placed between quartz plates. The highly air-sensitive compounds were studied by a technique[24] in which the sample was mixed with finely ground KBr. The resulting mixture was pressed between two layers of KBr. Low-temperature electronic spectra were obtained on an Air Products and Chemicals Inc. AC-2 Cryo-Tip refrigerator. Sample temperature was measured with a chromel–constantan thermocouple. The infrared spectra were obtained on a Perkin-Elmer 180 spectrometer in both KBr and CsI pressed pellets. In some instances the pressed pellet sandwich technique described above was used. The low-temperature spectra were obtained in a specially designed cell.[35] The magnetic measurements were made on either a Gouy or a Faraday balance[36] calibrated[37] with $HgCo(NCS)_4$. Powder X-ray diffraction patterns were obtained with a Straumannis camera and Ni-filtered Cu radiation. The Mössbauer spectral results between 78 K and room temperature were obtained on an Austin Science Associates spectrometer equipped with a room-temperature copper-matrix source. Results obtained at 4.2 K and lower used a Harwell Mössbauer spectrometer with a room-temperature rhodium-matrix source. Both spectrometers were calibrated with natural α-iron foil. For the 4.2 K and lower temperature spectra, the sample was immersed directly in liquid helium and its temperature was obtained by vapor pressure measurement. The National Bureau of Standards PARLOR computer program[38] was used to evaluate the paramagnetic Mössbauer spectral results. The magnetically ordered spectra were evaluated by using the FITH computer program developed by Lang and Dale.[39] Carbon, hydrogen, and nitrogen analyses were performed under a nitrogen atmosphere by Galbraith Laboratories, Inc., Knoxville, Tenn.

Results and Discussion

All of the compounds were prepared and handled in an oxygen-free nitrogen-atmosphere glovebox. This is essential to prevent decomposition of the bis compounds and all of the compounds when in solution. The tetrakis(pyridine) compounds are bright yellow and the bis(pyridine) compounds are pale yellow when pure and turn brown upon exposure to oxygen. The relative order of stability against oxidation for the complexes is Cl > Br ≈ NCS > I ≈ NCSe > NCO.

The results of a thermogravimetric study of the tetrakis complexes is reported elsewhere.[40] With the exception of the $Fe(py)_4(NCO)_2$, each of the compounds shows an endothermic pyridine weight loss to form the bis(pyridine) complexes. Our results are in substantial agreement with the previous results reported by Tominaga et al.[14,15] and others.[41] $Fe(py)_4(NCO)_2$ shows a continuous 68.2% endothermic weight loss above 55 °C corresponding to the loss of 4 mol of pyridine. This continuous weight loss indicates the instability of $Fe(py)_2(NCO)_2$ at temperatures above approximately 60 °C and the need for the use of lower temperature in its preparation.

Scheme I. X-ray Structural Correlations[a]

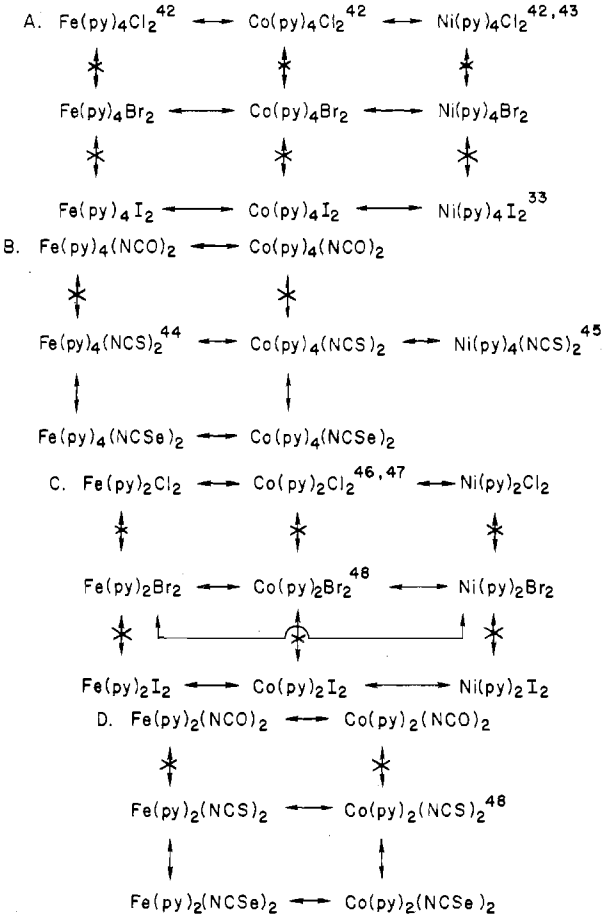

[a] Superscripts refer to text references to single-crystal structural work. ⟷ indicates isomorphous or structurally similar compounds; ⟷ indicates nonisomorphous compounds.

The X-ray powder diffraction patterns for all of the bis- and tetrakis(pyridine)iron(II) complexes and related complexes have been measured, and their *d* spacings are presented in Table II.[22] The X-ray *d* spacings indicate that several of these compounds are isomorphous or at least structurally similar to each other and to compounds whose single-crystal structures are known.[33,42-49] These correlations are presented in Scheme I.

The X-ray powder diffraction results for the tetrakis(pyridine) halide complexes indicate that complexes with a given halide are isomorphous. A distorted trans octahedral coordination geometry has been confirmed by single-crystal work on the chlorides[42] and on $Ni(py)_4I_2$[33] and is expected[28,50,51] for the bromide complexes. The single-crystal structure[44] of $Fe(py)_4(NCS)_2$ indicates that it is a distorted trans octahedral complex with a nitrogen-bonded thiocyanate. The remaining thiocyanate and selenocyanate complexes are at least structurally similar to this compound. $Fe(py)_2Cl_2$ is isomorphous at room temperature with α-$Co(py)_2Cl_2$ whose polymeric linear-chain distorted octahedral structure is known.[46,47] $Fe(py)_2Br_2$ is *not* isomorphous with $Co(py)_2Br_2$ which is known from X-ray[48] and spectroscopic[24,52-54] studies to be pseudo-

Table IV. Mössbauer Spectral Parameters[a]

compd	T, K	δ	ΔE_Q	Γ_1[b]	Γ_2[b]	e	compd	T, K	δ	ΔE_Q	Γ_1[b]	Γ_2[b]	e
$Fe(py)_2Cl_2$	room temp	1.08	0.57	0.25	0.25	4	$Fe(py)_4Cl_2$	room temp	1.06	3.08	0.31	0.31	3
	273	1.09	0.56	0.24	0.27	5		78	1.18	3.49	0.30	0.30	16
	244	1.10	0.55	0.25	0.26	7		4.2	1.10	3.42	0.24	0.24	
	233	1.11	0.55	0.26	0.26	7		1.32	1.05	3.48	0.28	0.31	
	195	1.13	0.56	0.20	0.26	3							
		1.15	1.14	0.26	0.24	5							
	78	1.21	1.25	0.34	0.32	9							
$Fe(py)_2Br_2$	room temp	1.03	0.82	0.32	0.32	3	$Fe(py)_4Br_2$	room temp	1.03	2.20	0.23	0.22	1
	230	1.06	1.10	0.27	0.25								
	78	1.15	1.18	0.27	0.27	6		78	1.09	2.86	0.25	0.26	5
	4.2	1.14	1.53	0.32	0.31			4.2	1.09	2.86	0.27	0.28	
	1.10	1.15	1.54	0.37	0.37								
$Fe(py)_2I_2$	room temp	0.76	0.94	0.31	0.27	1	$Fe(py)_4I_2$	room temp	0.99	0.33	0.24	0.28	2
	78	0.86	1.33	0.26	0.25	5		78	1.11	0.53	0.27	0.28	8
	4.2	0.95	1.81	0.30	0.31			4.2	1.12	0.65	0.26	0.25	
$Fe(py)_2(NCO)_2$	room temp	1.09	1.54	0.44	0.39	1.5	$Fe(py)_4(NCO)_2$	room temp	1.04	2.43	0.23	0.23	3
	78	1.21	2.16	0.39	0.44	4		78	1.16	2.62	0.28	0.28	20
								4.2	1.12	2.75	0.33	0.33	
$Fe(py)_2(NCS)_2$	room temp	1.02	2.60	0.26	0.26	6	$Fe(py)_4(NCS)_2$	room temp	1.05	1.54	0.25	0.24	2
	78	1.12	3.02	0.31	0.31	12		78	1.17	2.01	0.26	0.26	8
	4.2	1.16	2.56	0.38	0.38			4.2	1.16	1.90	0.35	0.32	
	1.28	1.14	2.80	0.32	0.32								
$Fe(py)_2(NCSe)_2$	room temp	1.00	2.83	0.27	0.28	1.5	$Fe(py)_4(NCSe)_2$	room temp	1.06	0.76	0.27	0.25	3
	78	1.13	3.14	0.28	0.27	5		78	1.17	0.91	0.26	0.26	4
	4.2	1.15	2.56	0.38	0.38								
	1.33	1.16	2.53	0.37	0.37								

[a] Relative to natural α-iron foil. [b] Full width at half-maximum for low-velocity line Γ_1 and high-velocity line Γ_2.

tetrahedral, whereas it is isostructural with octahedral[55] $Ni(py)_2Br_2$. The bis(pyridine) iodide complexes are all isomorphous or structurally similar. Unfortunately no single-crystal structure is available for the iodide complexes, but spectral studies indicate[24,28] that the complexes are pseudotetrahedral. The iron and cobalt thiocyanate and selenocyanate complexes are isostructural with $Co(py)_2(NCS)_2$ whose single-crystal structure[49] indicates a linear-chain polymeric octahedral geometry.

Magnetic Susceptibility Results. The results of our variable-temperature magnetic studies are given in Table III[22] and are in agreement with those available from previous studies.[7,8,16,17,21] The results are consistent with our formulation of these compounds as pseudooctahedral high-spin iron(II) compounds with a $^5T_{2g}$ ground state whose orbital degeneracy is removed by a low-symmetry crystal field. The temperature dependence of the magnetic moment for these complexes has been theoretically studied[56] as a function of electron delocalization, spin–orbit coupling, and distortion. The distortion is expressed in terms of Δ, the splitting between the d_{xy} and the d_{xz}, d_{yz} orbitals (or the $^5B_{2g}$ and ^5E_g states), and is positive if the d_{xy} orbital is lowest. Because this model is far from unique in its determination of the magnitude and sign of Δ,[16] no calculations have been attempted. However, in no instance are the results for the tetrakis complexes inconsistent with the predictions of this model. Earlier work[16] on $Fe(py)_4Br_2$ and $Fe(py)_4I_2$ has indicated that Δ is most likely positive, a result also confirmed for $Fe(py)_4(NCS)_2$ via single-crystal magnetic anisotropy measurements.[17]

The result is different for the bis(pyridine) complexes. At temperatures above ca. 100–150 K, the moments of these compounds are reasonable for distorted paramagnetic iron(II) complexes. However, in some instances, at lower temperatures, the magnetic moments increase dramatically with decreasing temperature. Low-temperature magnetic measurements[1-4] have revealed that $Fe(py)_2Cl_2$ and $Fe(py)_2(NCS)_2$ undergo a low-temperature metamagnetic transition to one-dimensional ferromagnetically ordered compounds with very weak bulk-antiferromagnetic coupling between chains. The critical ordering temperatures were found[4] to be 7 K for $Fe(py)_2Cl_2$ and 6 K for $Fe(py)_2(NCS)_2$. The temperature range studied for $Fe(py)_2Br_2$ would not be inconsistent with ordering at lower temperatures. However, the Mössbauer effect spectrum (see below) does not indicate any magnetic ordering above 1.1 K in this compound.

A plot of the magnetic moment and recriprocal susceptibility of $Fe(py)_2(NCO)_2$ is presented in Figure 1. Down to ca. 150 K the moment is typical of high-spin iron(II) complexes. Below this temperature, the moment begins to increase uniformly, as a result of the onset of ferromagnetic coupling through the bridging cyanate group between adjacent iron(II) sites in this polymer. This compound, which we believe to have only the nitrogen atom from the cyanate ligand bridging the metals, must have a rather high critical ordering temperature in order for these effects to be observed at ca. 100 K.

The magnetic properties of $Fe(py)_2(NCS)_2$ and $Fe(py)_2(NCSe)_2$ above ca. 100 K are normal for paramagnetic compounds. The increase in the magnetic moment for $Fe(py)_2(NCSe)_2$ below 100 K is an indication of the onset of ferromagnetic ordering. Mössbauer effect studies (see below) reveal that the ordering temperature for this compound is 6.7 K.

Evidence presented below indicates that $Fe(py)_2I_2$ is pseudotetrahedral. From its magnetic moment of 5.42 μ_B at 294 and 127.5 K it is not possible to distinguish between an octahedral or tetrahedral structure. The results are, however, consistent with the pseudotetrahedral coordination geometry.[57] As is observed for $Fe(py)_2I_2$, the magnetic moments for pseudotetrahedral iron(II) complexes typically range from 5.1 to 5.3 μ_B at room temperature and are independent of temperature.[58-63]

Mössbauer Effect Spectral Studies. The Mössbauer spectral parameters for the bis- and tetrakis(pyridine) complexes are presented in Table IV. The results obtained for the tetrakis(pyridine) complexes are typical of high-spin distorted octahedral iron(II) compounds and are in general agreement with previous reports.[6,12,13,21] In no instance is any magnetic ordering observed in these complexes down to the lowest temperature studied. The essentially identical isomer shifts observed for the three pseudohalide tetrakis complexes are consistent with the expected N-bonding coordination of the pseudohalide. The decrease in the room-temperature isomer

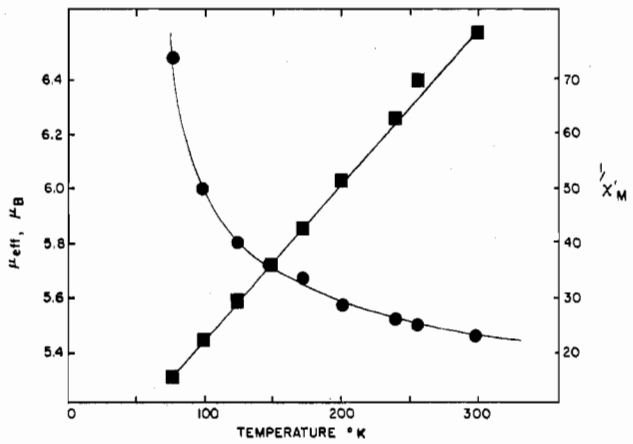

Figure 1. Temperature dependence of the recriprocal molar susceptibility and magnetic moment for $Fe(py)_2(NCO)_2$.

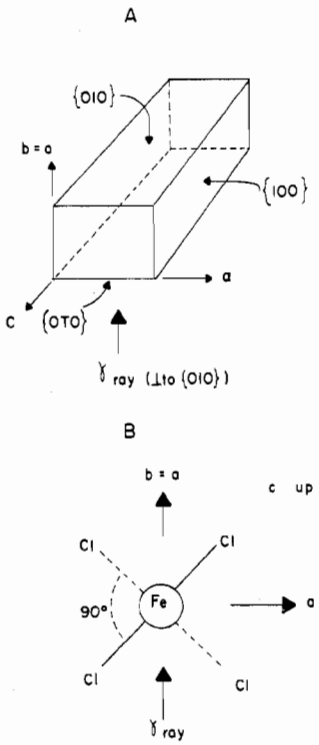

Figure 2. Crystal morphology (A) and molecule orientation (B) in $Fe(py)_4Cl_2$.

shift for the halide complexes reflects an increasing s-electron density at the iron nucleus[64,65] because of increased ligand σ donation and retrodative π bonding from filled iron orbitals to vacant ligand orbitals. The iodide with the highest covalency and lowest electronegativity has the lowest isomer shift. In most instances, the quadrupole splitting increases with decreasing temperature.[65]

The crystal structure[42] of $Fe(py)_4Cl_2$ reveals that this molecule has 222 point symmetry at the iron site. The symmetry is, however, very close to tetragonal and for the purposes of this paper, the molecule will be assumed to have a tetragonal axis coincident with the chlorine–chlorine vector. The crystals grow as rectangular prisms with a long c axis and the morphology shown in Figure 2A. The orientation of the pseudotetragonal Cl–Fe–Cl molecular axis to the crystallographic tetragonal c axis is shown in Figure 2B. This pseudotetragonal molecular axis is always oriented at 45° to the crystalline a or b axes. Because of the needle-like nature of the crystals, the c axis will always be essentially parallel with any surface upon which the crystals are placed. If the

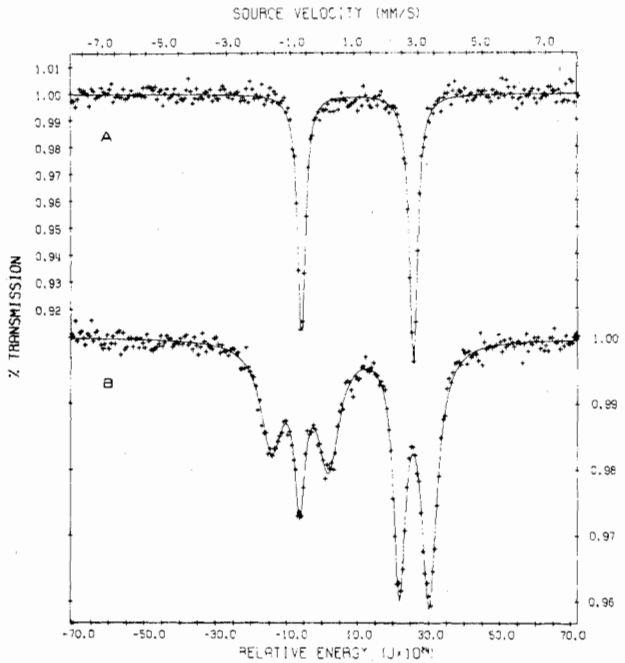

Figure 3. Mössbauer effect spectrum of polycrystalline $Fe(py)_4Cl_2$ at 1.32 K in (A) a zero field and (B) in a 0.4-T applied transverse magnetic field.

Mössbauer γ-ray direction is normal to this surface, the angle, θ, between the γ-ray and the pseudotetragonal molecular axis will always be 45° (unless some crystals are on edge) and will be independent of the orientation of the crystallographic c axis on the surface. In this case, the two components of a quadrupole-split doublet should not have equivalent intensity but should be in the ratio of 0.777 with the $m_I = \pm^1/_2$ to $m_I = \pm^3/_2$ component having the highest intensity.[65] This ratio will be the same even if some crystals are on edge because for each molecular pseudotetragonal axis at θ, there will be another site with the axis at $\theta - 90°$ and the averaged intensity ratio will be 0.777. However, if the γ-ray is parallel to the crystalline c axis, the value of θ is 90° for all iron sites and the ratio would be 1.67 with the $m_I = \pm^1/_2$ to $m_I = \pm^1/_2$ component having the highest intensity.[65] These intensity ratios should be independent of temperature.

Because of this combination of crystal morphology and molecular orientation, it is possible to determine the sign of the principal component of the electric field gradient tensor, V_{zz}, with a polycrystalline sample. The quadrupole-split Mössbauer spectrum of polycrystalline $Fe(py)_4Cl_2$ invariably has a high-velocity component of higher intensity with a typical intensity ratio of 0.82 to 0.84.[66] Because the high-velocity component is more intense, V_{zz} must be positive. This conclusion is further supported by the splitting observed in $Fe(py)_4Cl_2$ in a magnetic field, as is illustrated in Figure 3 at 1.35 K in a 0.4-T applied field. The appearance of the doublet at higher velocity is indicative of a positive V_{zz}.[67] The unusual intensity pattern observed in the lower velocity triplet is a result of the orientation effect described above. This and the large magnitude of the magnetic splitting observed in this compound will be discussed in a later paper.[68]

Unfortunately, the crystal structure of $Fe(py)_4Br_2$ is not known, but it is isomorphous with $Ni(py)_4Br_2$ which is orthorhombic with the *Pnam* space group.[69] Hence, it is not possible to determine the sign of V_{zz} from powder data as described above. The low-velocity line is, however, always observed to have the lower intensity. The spectrum (Figure 4) in a 6-T applied field at 4.2 K reveals a doublet at higher velocity and a triplet at lower velocity and is indicative of a positive V_{zz}. In this instance, we assume that V_{zz} is parallel

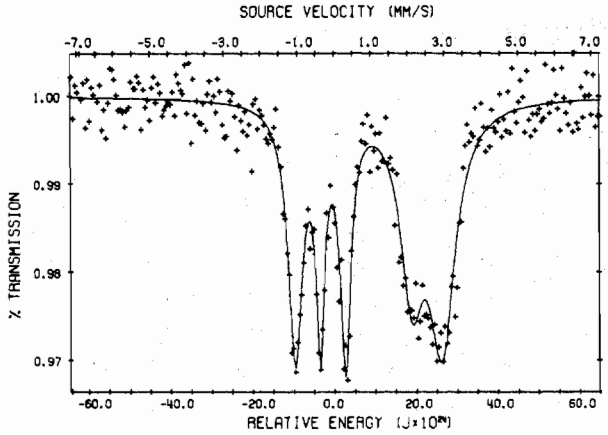

Figure 4. Mössbauer effect spectrum of polycrystalline $Fe(py)_4Br_2$ at 4.2 K in a 6-T applied transverse magnetic field.

with the Br–Fe–Br vector and that the distortion from molecular tetragonal symmetry is small.

The $Fe(py)_4I_2$ complex is isomorphous with $Ni(py)_4I_2$ and hence most likely is orthorhombic.[33] The small quadrupole interaction in this compound makes it difficult to determine the sign of the electric field gradient tensor by the application of a magnetic field. The results obtained at 4.2 K in a 6-T applied magnetic field are, however, most consistent with a positive V_{zz} which we assume is coincident with the I–Fe–I vector.

No structural data is available for $Fe(py)_4(NCO)_2$. Rather surprisingly this compound, which is paramagnetic at 4.2 K in the absence of an applied field, orders in an applied field of 6 T to give an internal hyperfine field of ca. 320 kOe. A single-crystal X-ray structure and a single-crystal applied-field Mössbauer effect study of this compound is in progress. The splitting of the six lines is consistent with a positive **EFG** tensor. We have tentatively chosen the cyanate N–Fe–N direction as coincident with the principal component, V_{zz}, of the **EFG** tensor.

The structure of $Fe(py)_4(NCS)_2$ has been reported by Søtofte and Rasmussen[44] as a monoclinic $C2/c$ crystal with two trans nitrogen-bonded thiocyanate groups. In this instance, the molecule displays a distinct distortion from tetragonal symmetry. This distortion manifests itself as two crystallographically distinct pyridine molecules with Fe–N distances of 2.247 and 2.272 Å. There is also a small distortion in the coordination angles from 90°. The magnetically perturbed Mössbauer spectrum of polycrystalline $Fe(py)_4(NCS)_2$ is shown in Figure 5.[22] Once again, the high-velocity component splits into a doublet at a 3-T applied field indicating a positive V_{zz}. In this instance, it is not possible to definitely assign the orientation of V_{zz} with respect to the molecular geometry, but we believe that the principal axis of the **EFG** tensor lies within a cone of 10° oriented along the Fe–N bond to the thiocyanate ligand.

No structural data is available for $Fe(py)_4(NCSe)_2$ and the small value of the quadrupole interaction makes the interpretation of the magnetically perturbed Mössbauer spectrum difficult. This compound is, however, isomorphous with $Fe(py)_4(NCS)_2$ and hence the same conclusions reached above will hold.

From the above experimental results we conclude that in all instances the principal component, V_{zz}, of the **EFG** tensor is positive and is most probably coincident with or close to the pseudotetragonal molecular axis. Divalent high-spin iron(II) has a $3d^6$ valence shell configuration in which the filled inner shells and the half-filled 3d orbitals will not contribute to the **EFG** tensor. The most important contribution to the **EFG** tensor will result from an unequal distribution of the "sixth" d electron among the t_{2g} orbitals or their admixture with the e_g orbitals in lower than tetragonal symmetry. This is the valence contribution to the **EFG** tensor. As the low-symmetry distortion approaches zero, the splitting of the t_{2g} orbitals and hence the quadrupole interaction will approach zero. It is for this reason that it is not possible to relate the magnitude of the quadrupole interaction to the ground-state orbital degeneracy.[70] An additional lattice contribution to the **EFG** tensor is also present in a complex of less than cubic symmetry. The lattice contribution is, however, usually small and opposite in sign to the valence contribution[71] and we have neglected it in the following discussion.

In contrast to the magnitude, it is possible to use the sign of the quadrupole interaction to determine the ground-orbital wave function for a given complex. This is certainly true if the complex has rigorous tetragonal molecular symmetry. Ingalls[71] has calculated the component of **EFG** which may be expected for each of the five 3d orbitals. For unmixed t_{2g} orbital wave functions, the d_{xy} orbital produces a positive component whereas both the d_{xz} and d_{yz} orbitals yield a negative term.[68] In strictly tetragonal compounds, $|V_{zz}| > |V_{yy}| = |V_{xx}|$ and V_{zz} must be coincident with the fourfold axis. Then a positive V_{zz} must correspond to a splitting of the $^5T_{2g}$ state with a resulting $^5B_{2g}$ ground state. This corresponds to the d_{xy} orbital which is lower in energy than the d_{xz} and d_{yz} orbitals which are of equivalent energy. A further reduction below tetragonal symmetry removes the equality of V_{yy} and V_{xx}, mixes the t_{2g} and e_g orbital wave functions, further splits the ^5E_g state, and removes the degeneracy of the d_{xz} and d_{yz} orbitals. Also, it is no longer certain that V_{zz} will be coincident with the "pseudotetragonal" axis.

With the above restrictions in mind, we offer the following analysis based upon the experimental observation that V_{zz} and ΔE_Q are positive for each of the tetrakis(pyridine) complexes and our expectation that the magnitude of the distortion from tetragonal symmetry is small. The splitting of the t_{2g} orbitals results predominantly from a difference in the π-bonding interaction of these orbitals with the axial and equatorial ligands.[72] The shift in energy of the t_{2g} orbitals upon a π-bonding interaction with ligand orbitals may be represented as e_π. We must also distinguish bonding interactions with different ligands. Hence, $e_{\pi X}$ will represent the interaction with the halide or N-bonded pseudohalide and $e_{\pi py}$ the interaction with pyridine. The use of the angular overlap model scaling factors[73] then yields the following energy expressions for the t_{2g} orbitals for a strictly tetragonal splitting in the tetrakis(pyridine) complexes:

$$d_{xz}, d_{yz}: \quad 2(e_{\pi X} + e_{\pi py})$$

$$d_{xy}: \quad 4e_{\pi py}$$

The tetragonal splitting is then defined as Δ with a positive value corresponding to the d_{xy} orbital lowest in energy.[56] Then for the tetrakis(pyridine) complexes, the splitting is given by (1). Because V_{zz} is positive for each of the tetrakis complexes,

$$\Delta_{tetrakis} = 2(e_{\pi X} - e_{\pi py}) \quad (1)$$

we know that $\Delta_{tetrakis}$ must be positive and are forced to conclude that $|e_{\pi X}| > |e_{\pi py}|$. If $e_{\pi py}$ is constant in each of the tetrakis(pyridine) complexes, then the magnitude of $\Delta_{tetrakis}$ may be related to the different values of $e_{\pi X}$. This assumption is supported by the apparent constancy of the Fe–N bond distance which is 2.23 Å in $Fe(py)_4Cl_2$[42] and 2.25 Å in $Fe(py)_2(NCS)_2$.[44]

Although it is possible to calculate the value of Δ from the temperature dependence of the quadrupole interaction, we choose not to do so because it is difficult to determine the magnitude of $q_{lattice}$, the effect of spin–orbit coupling, and the magnitude of low-symmetry distortion.[71,74] In addition, our

Table V. Mössbauer Effect Study of the Tetrakis to Bis Transformation[a]

product	T, K	reactant ΔE_Q	reactant δ	intermediate ΔE_Q	intermediate δ	product ΔE_Q	product δ	% product
$Fe(py)_2(NCSe)_2$	78	0.91	1.17					0
	78	0.89	1.17			3.08	1.14	15
	78	0.89	1.18			3.09	1.14	46
	78					3.10	1.13	100
$Fe(py)_2(NCO)_2$	room temp	2.43	1.04					0
	78	2.62	1.16					0
	78	2.64	1.16	1.52	1.16			14[b]
	78	2.62	1.16	1.65	1.19			50[b]
	78	2.58	1.14	1.60	1.19			73[b]
	78			1.73	1.21	2.33	1.21	28
	78			1.57	1.21	2.27	1.23	64
	78					2.16	1.21	100
	room temp					1.54	1.09	100

[a] All data in mm/s relative to natural α-iron foil. [b] Percent of intermediate present.

data set is too limited to be useful. Instead, we note that the relative magnitude of $e_{\pi X}$ is related to the magnitude of the positive quadrupole interaction[71] at a fixed temperature. By using the 78 K Mössbauer effect data, we conclude that

$$e_{\pi Cl} > e_{\pi Br} \gtrsim e_{\pi NCO} > e_{\pi NCS} > e_{\pi NCSe} > e_{\pi I} \approx e_{\pi py}$$

In other words, the chloride ion is most effective in destabilizing the d_{xz} and d_{yz} orbitals relative to the d_{xy} orbitals. Thus, the π bonding is most effective between the chloride orbitals and the metal orbitals and is least effective for the pyridine and iodine orbitals.

This same conclusion has resulted from the detailed analysis of the single-crystal magnetic anisotropy in $Fe(py)_4Cl_2$, $Fe(py)_4Br_2$, and $Fe(py)_4(NCS)_2$.[17,51] In this analysis the pyridine ligand is found to provide a small but definite π-donating effect upon the metal. In contrast, this analysis predicts that the bonding interaction of the bromide is somewhat stronger than the interaction with chloride. This difference may be a result of the fundamentally different type of measurement and highly different assumptions used in the analysis.[75] An optical study[76] of several tetragonal chromium(III) complexes has indicated that $e_\pi Cl > e_{\pi Br}$. Another study,[77] using thermodynamic data, indicates that the π-bonding ability of pyridine and substituted-pyridine ligands is somewhat smaller than that of the thiocyanate ligand. The relationship between ligand pK_b and the Zn–N bond length in a pseudotetrahedral series of pyridine and substituted-pyridine complexes of stoichiometry ZnL_2Cl_2 has led Steffen and Palenik[78] to conclude that the π-bonding effect of these ligands is minimal.

Our results now allow us to evaluate the π-bonding ability of the N-bonded pseudohalides relative to the halides and pyridine. Surprisingly, iodide is quite close to but probably somewhat greater than the pyridine in its π-bonding ability. It is interesting to note that, with the exception of the position of the bromide, the ligand π-bonding effects are in the same order as the group ligand electronegativities proposed by Hollebone.[79]

The preparation of the bis(pyridine) complexes may be divided into three types. $Fe(py)_2Cl_2$ and $Fe(py)_2Br_2$ complexes may be prepared directly from pyridine and the iron halide. In a second type of preparation, a thermolytic technique, the tetrakis(pyridine) complex is converted directly to the bis(pyridine) complex and no intermediate complex is found. This behavior is observed for the iodide, thiocyanate, and selenocyanate complexes and is illustrated in Figure 6[22] for $Fe(py)_2(NCSe)_2$. The consistency of the Mössbauer parameters for each component of the mixture (see Table V) indicates that the tetrakis(pyridine) complex is converted directly to the bis(pyridine) complex and that no intermediate is formed. In the third type of behavior, found in the thermolytic preparation of $Fe(py)_2(NCO)_2$, an intermediate species

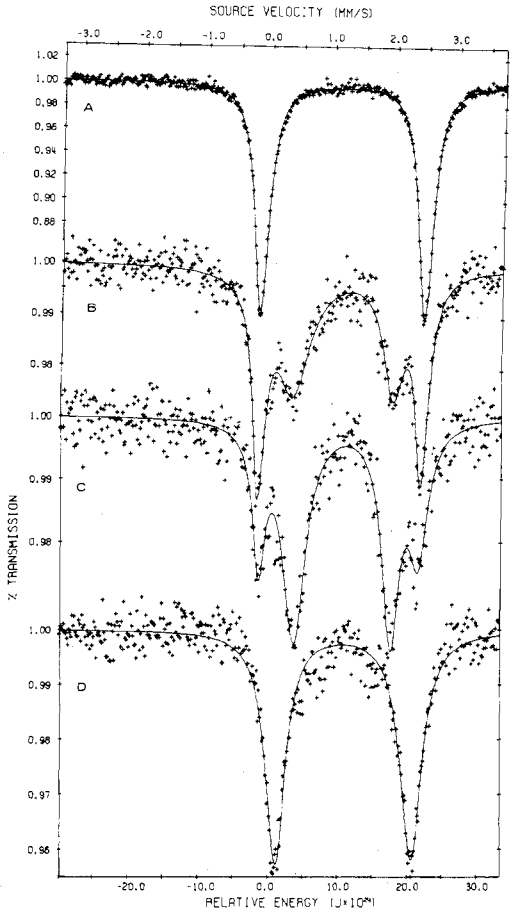

Figure 7. Mössbauer effect spectra obtained at 78 K illustrating the transformation of (A) pure $Fe(py)_4(NCO)_2$ via (B, C) intermediate $Fe(py)_3(NCO)_2$ to (D) pure $Fe(py)_2(NCO)_2$.

is observed. The Mössbauer effect data for this transformation is presented in Table V and the observed spectra are shown in Figure 7.

A study of Table V reveals that there are only slight changes in the Mössbauer parameters for $Fe(py)_4(NCO)_2$ when the weight loss has been small. The second component in these spectra exhibits a smaller quadrupole interaction and a slightly larger chemical isomer shift. The area of this component is proportional to the weight loss. Because this intermediate is found in the thermolysis between $Fe(py)_4(NCO)_2$ and $Fe(py)_2(NCO)_2$, we conclude that it is most likely $Fe(py)_3(NCO)_2$ and propose the dimeric structure I. The slight increase in the chemical isomer shift for I relative to $Fe(py)_4(NCO)_2$ is consistent with the loss of pyridine and the

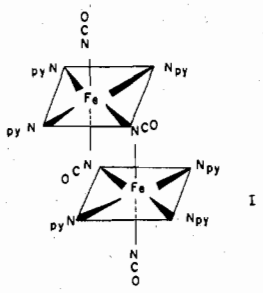

I

addition of the two bridging cyanates. At first it seems surprising that the dimer has a smaller quadrupole interaction and a smaller **EFG** at the iron site. However, if we assume that the π-bonding effect of the terminal bridged cyanate group is significantly reduced in this bridging configuration such that the inequality $e_{\pi NCO} > e_{\pi^{**}NCO} \gtrsim e_{\pi py}$ holds, then the energy of the t_{2g} orbitals is given by the following, where the pseudotetragonal axis is defined by the iron to monodentate NCO bond. (In these and subsequent expressions, the bonding atoms in bridging ligands are indicated with an asterisk; hence **NCO indicates that nitrogen is the only bridging atom.)

$$d_{xz}: \quad e_{\pi py} + 2e_{\pi^{**}NCO} + e_{\pi NCO}$$

$$d_{yz}: \quad 2e_{\pi py} + e_{\pi^{**}NCO} + e_{\pi NCO}$$

$$d_{xy}: \quad 3e_{\pi py} + e_{\pi^{**}NCO}$$

In this instance, the splitting of the t_{2g} orbitals for I would be given by (2) for the d_{xy} and d_{yz} orbitals and by (3) for the d_{xy} and d_{xz} orbitals. As the value of $e_{\pi^{**}NCO}$ approaches $e_{\pi py}$, $\Delta_{I,1}$ approaches $\Delta_{I,2}$ and the splitting of the t_{2g} orbitals approaches Δ_I as given in (4). This value is half the value calculated for

$$\Delta_{I,1} = e_{\pi NCO} - e_{\pi py} \tag{2}$$

$$\Delta_{I,2} = e_{\pi NCO} + e_{\pi^{**}NCO} - 2e_{\pi py} \tag{3}$$

$$\Delta_I = e_{\pi NCO} - e_{\pi py} \tag{4}$$

the splitting in the tetrakis complex in eq 1. The value we observed for the quadrupole interaction in the intermediate is ca. 60% of that observed in $Fe(py)_4(NCO)_2$ indicating that the π-bonding effect of the cyanate group is significantly reduced in the bridging configuration and is similar to $e_{\pi py}$.

As the vacuum thermolysis at 55 °C of the cyanate complex continues, the intermediate is slowly converted to the bis complex (Figure 7). The $Fe(py)_2(NCO)_2$ complex is very sensitive to oxidation, and small traces of iron(III) are sometimes observed at ca. 0.5 mm/s in the Mössbauer spectrum. The results given in Table V for $Fe(py)_2(NCO)_2$ have been reproduced five times, twice by thermolysis under hydrogen and three times by vacuum thermolysis.

The isomer shift values for each of the bis complexes are typical of high-spin pseudooctahedral iron(II)[65] and are similar to the shifts observed for the tetrakis complexes. Hence, the comments presented above also apply for the bis complexes. The $Fe(py)_2Cl_2$ complex is isomorphous with the α-$Co(py)_2Cl_2$ complex at room temperature and undergoes a transition[1] at ca. 195 K to a structure similar to γ-$Co(py)_2Cl_2$.[47] In this low-temperature monoclinic structure, a distinct asymmetry is observed in the Co–Cl bond distances of the bridging chloride ions in the linear-chain structure. Hence, although V_{zz} is known[5] to be positive for this complex, it is not possible with polycrystalline samples to determine the orientation of the principal axis of the **EFG** tensor relative to the molecular bonding framework. Thus, it is not possible to determine the symmetry of the ground-state wave function.

The $Fe(py)_2(NCS)_2$ and $Fe(py)_2(NCSe)_2$ complexes are both isomorphous with $Co(py)_2(NCS)_2$ whose monoclinic linear-chain crystal structure has been reported.[49] $Fe(py)_2(NCS)_2$ has a positive V_{zz}, but again it is not possible, because of the low symmetry of the coordination sphere, to determine the orientation of V_{zz} and the ground-state orbital function for these complexes. As a result, it will not be possible to attempt an analysis of the π-bonding effects based on the quadrupole splitting as was presented above for the tetrakis(pyridine) complexes. The quadrupole interaction in the bis(pyridine) pseudohalides is significantly larger than in the bis(pyridine) halide and tetrakis(pyridine) thiocyanate and selenocyanate complexes. This larger splitting is a result of the bonding of the sulfur and selenium atoms in the coordination sphere of these complexes. It seems reasonable that the **EFG** tensor resulting from the $FeN_2N_2'S_2$ or $FeN_2N_2'Se_2$ coordination sphere would be larger than that resulting from the FeN_2X_4 (X represents the bridging halide) coordination sphere, even if the halide bridging is asymmetric. This also explains the larger value of the quadrupole interaction in $Fe(py)_2(NCS)_2$ and $Fe(py)_2(NCSe)_2$ as compared with the respective tetrakis complexes. $Fe(py)_2(NCO)_2$ which has only coordinated nitrogen atoms has a smaller quadrupole interaction than the other bis(pyridine) pseudohalide complexes and $Fe(py)_4(NCO)_2$. Bonding of the terminal bridging cyanate ligand in $Fe(py)_2(NCO)_2$ resembles more closely the bonding of pyridine than does the monodentate N-bonded cyanate in $Fe(py)_4(NCO)_2$. This is consistent with the inequality $e_{\pi NCO} > e_{\pi^{**}NCO} \gtrsim e_{\pi py}$ discussed above and the smaller quadrupole interaction found in $Fe(py)_2(NCO)_2$.

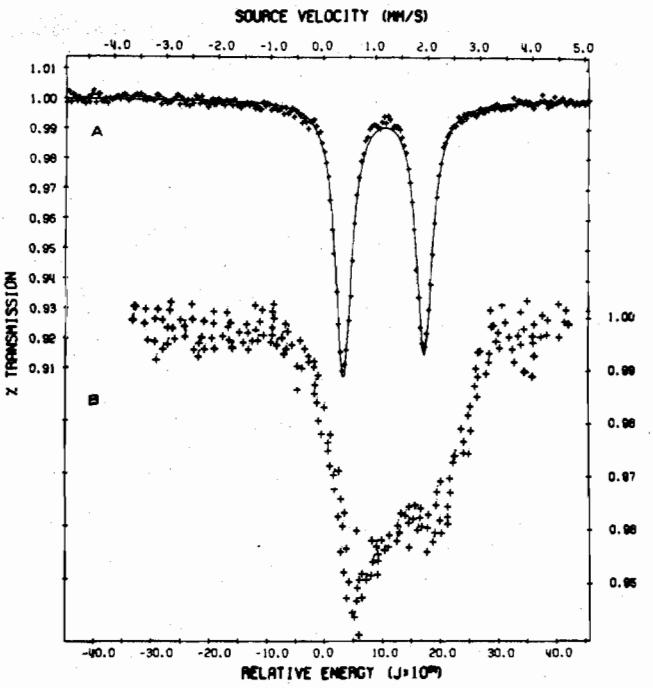

Figure 8. Mössbauer effect spectrum of (A) $Fe(py)_2Br_2$ at 1.1 K and (B) at 4.2 K in a 6-T applied field.

As we have reported earlier,[1] there is a large increase in the quadrupole splitting of $Fe(py)_2Cl_2$ between 233 and 78 K. The increase in ΔE_Q is associated with a reversible phase transition from a high-temperature symmetric bridged phase to a low-temperature asymmetric bridged phase. Both phases are present at 195 K. In contrast, $Fe(py)_2Br_2$ does not show any dramatic increase in ΔE_Q between room temperature and 1.10 K (see Figure 8). Apparently no structural change occurs above 78 K—the temperature dependence is probably a Boltzmann population effect. The increase in ΔE_Q between 78 and 4.2 K could indicate a structural change, but a more detailed study of the temperature dependence of ΔE_Q between 4.2 and 78 K is required to determine this. $Fe(py)_2Br_2$ does

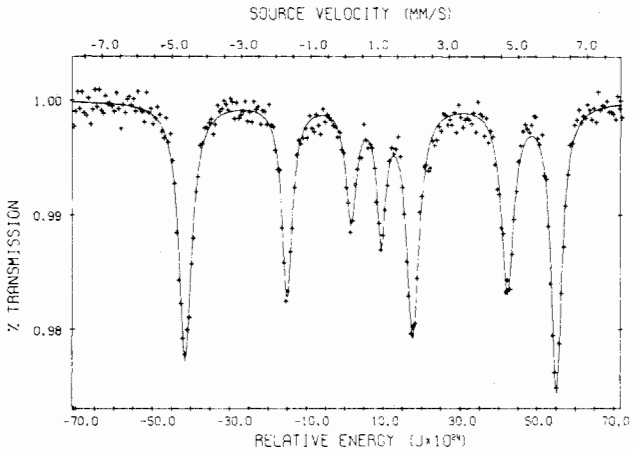

Figure 9. Mössbauer effect spectrum of $Fe(py)_2(NCSe)_2$ at 1.33 K.

not spontaneously order at temperatures above 1.10 K. Apparently the transfer of electron spin potential via the bridging bromide ion is very small. A similar depression of the ordering temperature in $Ni(py)_2Br_2$ has been found in specific heat studies.[80] In addition, no ordering is observed even in the presence of a 6-T applied field where the spectrum (Figure 8) is typical of a paramagnetic compound.

The Mössbauer spectra of $Fe(py)_2(NCS)_2$ and $Fe(py)_2(NCSe)_2$ indicate that these compounds are spontaneously ordered at 4.2 K and lower as shown in Figure 9 for $Fe(py)_2(NCSe)_2$ at 1.33 K. Essentially the same spectrum is observed at 4.2 K and for $Fe(py)_2(NCS)_2$ at 4.2 and 1.28 K. The internal hyperfine field for both compounds at 4.2 K and below is ca. 270 kOe, a value in good agreement with the value obtained for $Fe(py)_2(NCS)_2$ at 4.2 K.[2] A preliminary estimate of the isomer shift and quadrupole interaction in these spectra has been obtained by using the approach of Lang and Dale[39] and the results are presented in Table IV. The theoretical fits indicate an anisotropic **g** and **A** tensor. This is consistent with the high magnetic anisotropy predicted and observed for these pseudo-one-dimensional metamagnetic systems[3] and with the low internal hyperfine field observed in these compounds. A compound with an $S = 2$ ground state would have a spin contribution to the internal hyperfine field of ca. 440 kOe.[65,81-83] This would be reduced by a high magnetic anisotropy and by an orbital contribution to the hyperfine field. Both compounds exhibit a decrease in ΔE_Q below 78 K which we believe may result from a small structural change at or near the ordering temperature.

The X-ray and electronic spectral results indicate that $Fe(py)_2I_2$ has a pseudotetrahedral structure. The lower coordination number for a tetrahedral iron(II) complex leads to a lower isomer shift (0.70–0.90 mm/s) than in octahedral complexes.[58,59,61,63,84] The Mössbauer parameters presented in Table IV for $Fe(py)_2I_2$ provide further evidence for the pseudotetrahedral structure. The quadrupole interaction is typical of pseudotetrahedral iron(II) and indicates a splitting of the $d_{x^2-y^2}$ and d_{z^2} orbitals of the order of 100 cm^{-1} by the low-symmetry component of the ligand field.[84] As expected, this compound shows no indication of ordering at 4.2 K.

Electronic Spectral Results. The electronic spectral data for each of the complexes measured at various temperatures are presented in Table VI along with band assignments. Standard error estimation and propagation procedures were used.[24,85] The pseudooctahedral electronic spectra exhibit either two weak bands in the near-infrared and visible regions or two poorly resolved bands (where the second band is usually observed as a low-energy shoulder). In each instance, the spectrum of the bis complex is quite different from that of the tetrakis complex. For instance, in both $Fe(py)_4(NCS)_2$ and

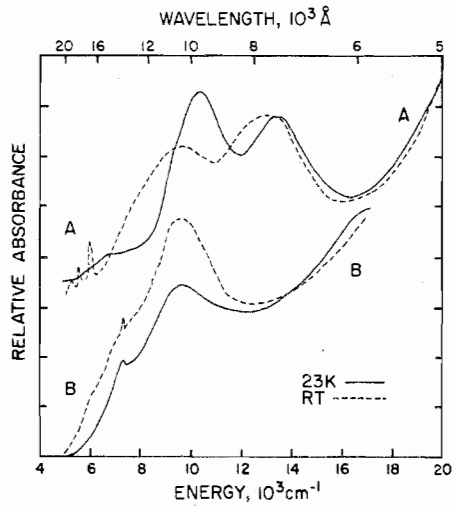

Figure 12. Electronic absorption spectra measured at room temperature and 23 K for (A) $Fe(py)_4(NCO)_2$ and (B) $Fe(py)_2(NCO)_2$.

$Fe(py)_4(NCSe)_2$ the two lines are poorly resolved with a splitting of ca. 1500 cm^{-1}, whereas in the bis complexes, the two lines are well resolved with a splitting of ca. 5500 cm^{-1} (see Figure 10[22]). A similar trend is found for the tetrakis- and bis(pyridine) chloride and bromide complexes as is illustrated in Figure 11.[22] The reverse trend is found for $Fe(py)_4(NCO)_2$ and $Fe(py)_2(NCO)_2$ as shown in Figure 12.

The electronic spectra may be understood by using two basic approaches. First, the splitting in the spectra may be related to the σ bonding of the ligands by using either the McClure[72] approach or the angular overlap model.[73,85] Second, the magnitude of the electronic spectral bands may be related via ligand field theory to the spectrochemical potential for the various ligands.

For the tetrakis(pyridine) complexes, the energy of the σ-bonding orbitals is

$$d_{x^2-y^2}: \quad 3e_{\sigma py}$$

$$d_{z^2}: \quad 2e_{\sigma X} + e_{\sigma py}$$

where notation similar to that used above is retained. The splitting in these orbitals, δe_σ, is given by eq 5. For the

$$\delta e_\sigma = E(d_{x^2-y^2}) - E(d_{z^2}) = -(\nu_1 - \nu_2) = 2(e_{\sigma py} - e_{\sigma X}) \quad (5)$$

bis(pyridine) complexes, similar expressions are obtained, except that, in order to maintain a consistent sign convention (in the presence of the reversed band assignments, see Table VI), the reverse definition of the splitting energy is used. Hence, for the bis complexes, the energy of the σ-bonding orbitals is

$$d_{z^2}: \quad 2e_{\sigma py} + e_{\sigma X}$$

$$d_{x^2-y^2}: \quad 3e_{\sigma X}$$

The splitting in the electronic spectra of the bis complexes is given by (6) and the expression is the same as for the tetrakis

$$\delta e_\sigma = E(d_{z^2}) - E(d_{x^2-y^2}) = \nu_1 - \nu_2 \quad (6)$$

$$= 2(e_{\sigma py} - e_{\sigma X}) \quad (5)$$

complexes (5). Values of δe_σ at room temperature and at 23 K are given in Table VII.

If we assume that pyridine has a constant given value for its contribution to the σ bonding in all of the complexes, then relative e_σ values for each of the anions may be calculated. If we first assume a zero value for $e_{\sigma py}$—making the pyridine

Table VI. Experimental Electronic Spectral Results[a]

compd	T, K	ν_1, $\rightarrow {}^5A_{1g}$	ν_2, $\rightarrow {}^5B_{1g}$	$\nu_1 - \nu_2$	ν_{av}
$Fe(py)_4Cl_2$[b]	300	8720 ± 100 sh	10520 ± 50	−1800 ± 80	9620 ± 80
	175	8720 ± 100 sh	10990 ± 50	−2270 ± 80	9850 ± 80
	127	8810 ± 100 sh	11110 ± 50	−2300 ± 80	9960 ± 80
	23	8850 ± 100 sh	11300 ± 50	−2450 ± 80	10070 ± 80
$Fe(py)_4Br_2$[b]	300	7690 ± 60	10870 ± 50	−3180 ± 60	9280 ± 60
	210	7900 ± 100	10990 ± 50	−3090 ± 80	9440 ± 80
	144	8000 ± 60	11230 ± 50	−3230 ± 60	9610 ± 60
	102	8030 ± 70	11230 ± 50	−3200 ± 60	9630 ± 60
	23	8060 ± 50	11360 ± 50	−3300 ± 50	9710 ± 50
$Fe(py)_4I_2$[b]	300	5950 ± 120	11300 ± 50	−5350 ± 90	8620 ± 90
	265	5950 ± 120	11430 ± 50	−5480 ± 90	8690 ± 90
	238	5990 ± 90	11430 ± 50	−5440 ± 70	8710 ± 70
	185	6210 ± 90	11630 ± 50	−5420 ± 70	8920 ± 70
	145	6290 ± 60	11760 ± 50	−5470 ± 60	9020 ± 60
	100	6370 ± 50	11900 ± 50	−5530 ± 50	9130 ± 50
	23	6450 ± 50	12050 ± 50	−5600 ± 50	9250 ± 50
$Fe(py)_4(NCO)_2$[b]	300	9430 ± 70	12580 ± 50	−3150 ± 60	11000 ± 60
	221	9760 ± 50	12940 ± 50	−3180 ± 50	11350 ± 50
	124	10020 ± 60	13160 ± 50	−3140 ± 60	11590 ± 60
	23	10260 ± 50	13240 ± 60	−2980 ± 60	11750 ± 60
$Fe(py)_4(NCS)_2$[b]	300	9880 ± 170 sh	11460 ± 60	−1580 ± 130	10670 ± 130
	250	9900 ± 150 sh	11490 ± 60	−1590 ± 110	10690 ± 110
	125	10230 ± 110 sh	11550 ± 60	−1320 ± 90	10890 ± 90
	23	10360 ± 120 sh	11450 ± 70	−1090 ± 100	10900 ± 110
$Fe(py)_4(NCSe)_2$[b]	300	9900 ± 170 sh	11360 ± 60	−1460 ± 130	10630 ± 130
	231	10109 ± 150 sh	11370 ± 70	−1270 ± 120	10730 ± 120
	23	10990 ± 170 sh	11620 ± 100	−630 ± 140	11300 ± 140
$Fe(py)_2Cl_2$[b]	300	9710 ± 50	5760 ± 50	3950 ± 50	7730 ± 50
	277	9660 ± 50	5780 ± 50	3880 ± 50	7720 ± 50
	100	9660 ± 50	5880 ± 50	3780 ± 50	7770 ± 50
	23	9660 ± 50	5880 ± 50	3780 ± 50	7770 ± 50
$Fe(py)_2Br_2$[c]	300	9520 ± 50	5180 ± 60	4340 ± 60	7350 ± 60
	215	9660 ± 50	5260 ± 60	4400 ± 60	7460 ± 60
	23	9710 ± 50	5320 ± 60	4390 ± 60	7515 ± 60
$Fe(py)_2(NCO)_2$[c]	300	9570 ± 70	7410 ± 120 sh	2160 ± 100	8490 ± 100
	140	9660 ± 70	7570 ± 100 sh	2090 ± 90	8610 ± 90
	115	9660 ± 70	7580 ± 100 sh	2080 ± 90	8620 ± 90
	80	9660 ± 70	7600 ± 100 sh	2060 ± 90	8630 ± 90
	23	9710 ± 70	7690 ± 120 sh	2020 ± 100	8700 ± 100
$Fe(py)_2(NCS)_2$[c]	300	12660 ± 70	7300 ± 50	5360 ± 60	9980 ± 60
	190	12990 ± 70	7410 ± 50	5580 ± 60	10200 ± 60
	145	13080 ± 70	7490 ± 50	5590 ± 60	10280 ± 60
	92	13160 ± 70	7550 ± 50	5610 ± 60	10350 ± 60
	23	13330 ± 60	7690 ± 50	5640 ± 60	10510 ± 60
$Fe(py)_2(NCSe)_2$[c]	300	12820 ± 90	7090 ± 70	5730 ± 80	9950 ± 80
	192	12990 ± 90	7250 ± 60	5740 ± 80	10120 ± 80
	129	13070 ± 70	7260 ± 70	5810 ± 70	10160 ± 70
	96	13160 ± 60	7520 ± 60	5640 ± 60	10340 ± 60
	23	13240 ± 60	7550 ± 60	5690 ± 60	10400 ± 60

[a] All data in cm^{-1}. [b] Measured in Flurolube mull. [c] Measured by KBr sandwich technique.[24]

Table VII. Variation in Ligand σ-Antibonding Effects and Crystal Field Effects[a]

compd	$\delta e_\sigma^{\text{room temp}}$	$\delta e_\sigma^{23\text{ K}}$	$e_{\sigma x}^{\text{room temp}}$	$e_{\sigma x}^{23\text{ K}}$	$e_{\sigma x}^{\text{room temp}}$	$e_{\sigma x}^{23\text{ K}}$	$e_{\sigma x}$	ρ_x[b]	$\delta\nu_{av}$
$Fe(py)_2(NCSe)_2$	5730 ± 80	5690 ± 60	−2860 ± 80	−2840 ± 60	1190 ± 170	1210 ± 160	e_{σ}*NCSe*	1340	450 ± 70
$Fe(py)_2(NCS)_2$	5360 ± 60	5640 ± 50	−2680 ± 60	−2820 ± 50	1370 ± 160	1230 ± 150	e_{σ}*NCS*	1340	530 ± 60
$Fe(py)_4I_2$	5350 ± 90	5600 ± 50	−2680 ± 90	−2800 ± 50	1370 ± 180	1250 ± 150	$e_{\sigma I}$	310	630 ± 70
$Fe(py)_2Br_2$	4340 ± 50	4390 ± 50	−2170 ± 50	−2200 ± 50	1880 ± 150	1850 ± 150	e_{σ}*Br*	680	160 ± 60
$Fe(py)_2Cl_2$	3950 ± 50	3780 ± 50	−1980 ± 50	−1890 ± 50	2070 ± 150	2160 ± 150	e_{σ}*Cl*	780	40 ± 50
$Fe(py)_4Br_2$	3180 ± 50	3300 ± 50	−1590 ± 50	−1650 ± 50	2460 ± 150	2400 ± 150	$e_{\sigma Br}$	640	430 ± 60
$Fe(py)_4(NCO)_2$	3150 ± 60	2980 ± 50	−1580 ± 60	−1490 ± 50	2470 ± 160	2560 ± 150	$e_{\sigma NCO}$	1500	750 ± 60
$Fe(py)_2(NCO)_2$	2160 ± 100	2020 ± 100	−1080 ± 100	−1010 ± 100	2970 ± 190	3040 ± 190	e_{σ}**NCO	970	210 ± 100
$Fe(py)_4Cl_2$	1800 ± 80	2450 ± 80	−900 ± 80	−1220 ± 80	3150 ± 170	2830 ± 170	$e_{\sigma Cl}$	810	450 ± 80
$Fe(py)_4(NCS)_2$	1580 ± 130	1090 ± 100	−790 ± 130	−540 ± 100	3260 ± 230	3510 ± 190	$e_{\sigma NCS}$	1340	230 ± 120
$Fe(py)_4(NCSe)_2$	1460 ± 130	630 ± 140	−730 ± 130	−320 ± 140	3320 ± 230	3730 ± 240	$e_{\sigma NCSe}$	1320	670 ± 140
			0	0	4050 ± 230	4050 ± 240	$e_{\sigma py}$		

[a] All data in cm^{-1}. [b] Room temperature values of the partial crystal field potential relative to $\rho_{py} = 2000$ cm^{-1} for the tetrakis compounds and $\rho_{py}' = 2400$ for the bis compounds (see text).

σ-bonding contribution the largest of all the ligands—then the relative values of $e_{\sigma X}$ may be calculated from eq 5 and 6. The resulting values and the specific symbols used for $e_{\sigma X}$ are given in Table VII. The actual value of $e_{\sigma py}$ may be determined as follows. It is known[73,87] that in an octahedral complex, the splitting of the σ- and π-bonding orbitals, ν, is given by the equation $\nu = 3e_\sigma - 4e_\pi$. When the degeneracy of these orbitals is further removed, as in a pseudooctahedral complex, the average splitting is given by eq 7, which would hold for our

$$\begin{aligned} \nu_{av} &= 3e_{\sigma av} - 4e_{\pi av} \\ &= 2e_{\sigma py} + e_{\sigma NCS} - 3e_{\pi py} - e_{\pi NCS} \end{aligned} \quad (7)$$

tetrakis(pyridine) complexes. Note that ν_{av} is the average value of $10Dq$ in these complexes (see below). If, for $Fe(py)_4(NCS)_2$, we use the value of $e_{\pi py}$ and $e_{\pi NCS}$ as determined by Gerloch et al.[17] and the values of $e_{\sigma NCS}^{room\ temp}$ and $\nu_{av}^{room\ temp}$ given in Table VI, it is possible to calculate a value of $e_{\sigma py}$, and hence the remaining relative values of $e_{\sigma X}$. The resulting values at room temperature and 23 K are given in Table VII where it is noted that $e_{\sigma py}$ is 4050 cm^{-1}. The values obtained at 23 K have assumed that $e_{\pi py}$ and $e_{\pi NCS}$ do not change with temperature. It is interesting that $e_{\sigma py}$ does not change with temperature. Our value of $e_{\sigma py}$ is in surprisingly good agreement with the values of ca. 3700 ± 500 cm^{-1} obtained by Gerloch et al.[17] from single-crystal magnetic anisotropy studies on $Fe(py)_4(NCS)_2$. Our value for $e_{\sigma Cl}$ is also in good agreement with the value obtained from a similar study[51] of $Co(py)_4Cl_2$. The value of $e_{\sigma Br}$ of 2460 cm^{-1} is, however, significantly lower than the value of 3000 cm^{-1} obtained from the magnetic study[51] of $Co(py)_4Br_2$. Our results indicate that the electronic spectra of these compounds are more sensitive to changes in the e_σ parameters than are the magnetic measurements.

The results presented in Table VII indicate that the value of e_σ, and hence the σ-antibonding effect of the ligands, increases with descent down this table. From these results, we can see that the bidentate bridging anions are the poorest σ-donor ligands while the monodentate anions are the best and most like pyridine. The trend $e_{\sigma NCSe} > e_{\sigma NCS} > e_{\sigma NCO}$ is reasonable because the electron-donating ability of the bonding nitrogen atom would decrease as the electronegativity of the group 6A atom increases. The trend for the bridging pseudohalide ligands is more difficult to understand. The failure of the NCO ligand to utilize the oxygen atom in its bridging is probably a result of the high electronegativity and small size of oxygen. The trend for the halides, which is the opposite of what would be expected on the basis of an electronegativity argument, must be a result of a more effective orbital overlap for the chloride ligand and poorer overlap for the iodide. There is no real change in $e_{\sigma X}$ with decreasing temperature, indicating that, as expected, the changes in σ bonding are rather insensitive to temperature. Indeed, no change is observed in $Fe(py)_2Cl_2$ even though this material is known[1] to undergo a phase change at ca. 195 K.

The values of ν_{av} given in Table VI indicate the total crystal field potential that the pyridine ligands and various anions impose upon the metal. In order to obtain relative quantitative values for the various anions, we have assigned a partial crystal field potential ρ_X to each of the ligands such that their sum is the observed ν_{av}. If we assume the same value of ρ_{py} for the bis and tetrakis compounds, the values obtained for the bridging chloride and bromide ions were higher than for the singly bonded chloride and bromide. Because this seems unreasonable, we have chosen a value of ρ_{py}' for the bis compounds which is 20% higher than ρ_{py} in the tetrakis compounds. This difference seems reasonable in view of the shorter metal–pyridine bond distance[42] in the bis complexes when compared with the tetrakis complexes. This assumption gives values for the partial crystal field potential of the bridging halides which are slightly lower than those of the terminal halides. In addition, the values for the terminal and bridging thiocyanate and selenocyanate anions are essentially the same. The relative room-temperature values of these partial crystal field potentials are presented in Table VII. The order of increasing crystal field potential is given as $\rho_I < \rho_{Br} \lesssim \rho_{*Br*} < \rho_{*Cl*} \lesssim \rho_{Cl} < \rho_{**NCO} < \rho_{NCSe} \sim \rho_{NCS} = \rho_{*NCS*} = \rho_{*NCSe*} < \rho_{NCO} < \rho_{py}$, an order that parallels the spectrochemical series. It is interesting that the bridging cyanate ligand with its three-center bond has a lower crystal field potential than the terminal cyanate ligand.

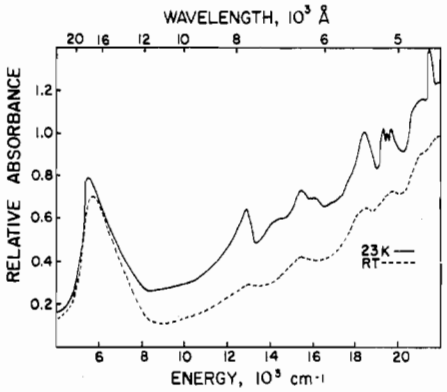

Figure 13. Electronic absorption spectra measured at room temperature and 23 K for $Fe(py)_2I_2$.

Table VIII. Electronic Spectral Results for $Fe(py)_2I_2$

exptl, cm^{-1}		calcd for $B = 800$, $C = 4B$	assign
room temp	23 K		
5 760 ± 70	5 580 ± 70	5 580	$^5E \rightarrow {}^5T_2$
13 100 ± 80	12 990 ± 70	12 800	$^5E \rightarrow {}^3T_1(^3H)$
15 560 ± 50	14 500 ± 60 15 380 ± 50	15 200	$^5E \rightarrow {}^3E(^3H)$
	16 130 ± 50	16 000	$^5E \rightarrow {}^3T_1(^3H)$
18 590 ± 50	18 420 ± 50	18 400	$^5E \rightarrow {}^3A_2(^3F)$
19 800 ± 50	19 360 ± 25 19 520 ± 50 19 720 ± 25	19 680	$^5E \rightarrow {}^3T_1(^3F)$
21 280 ± 100	20 900 ± 50	20 800	$^5E \rightarrow {}^3T_2(^3F)$

We have defined the shift in ν_{av} with decreasing temperature as $\delta\nu_{av} = \nu_{av}^{23\ K} - \nu_{av}^{300\ K}$, and have presented the results in Table VII. All of our compounds, with the possible exception of $Fe(py)_2Cl_2$, show a positive value of $\delta\nu_{av}$ and hence an increase in the crystal field potential with decreasing temperature. A study of the temperature shift of the individual absorption lines indicates that each line increases an equivalent amount with decreasing temperature, yielding values essentially the same as $\delta\nu_{av}$. This isotropic thermal increase in the energy of ν_1 and ν_2 could result either from a thermal contraction of the unit cell or from a change in the Boltzmann population of the ^5E_g state (or the $^5A_{1g}$ and $^5B_{1g}$ states in lower than axial symmetry) which arises from the $^5T_{2g}$ state in octahedral symmetry. Because we have no quantitative values for $\Delta_{tetrakis}$—or the equivalent splitting in the bis complexes—it is difficult to determine the magnitude of the shift which results from changes in the Boltzmann population. This contribution may be significant when $\Delta_{tetragonal}$ is less than ca. 250 cm^{-1}. For a larger splitting, the change in Boltzmann population is insignificant between 300 and 23 K. We believe that the increase in ν_{av} with decreasing temperature probably results from an essentially isotropic thermal contraction of the unit cell.

The electronic spectrum of $Fe(py)_2I_2$ is shown in Figure 13 and tabulated in Table VIII. The spectrum is indicative of low-symmetry pseudotetrahedral coordination. The $^5E \rightarrow {}^5T_2$

Table X. Infrared Spectral Assignments[a]

compd	ν_{N-CX}	ν_{NC-X}	δ_{NCX}	$\nu_{Fe-X,NCX}$	ν_{Fe-Npy}	$\nu_{Fe-X(CN)}$	$2\delta_{NCX}$
$Fe(py)_4Cl_2$				237 m	225 s		
$Fe(py)_4Br_2$				195 s	225 s		
$Fe(py)_4I_2$				196 s[b]	213 s		
$Fe(py)_4(NCO)_2$	2190 vs 2142 sh	1329 s	628 s	308 s	201 s		1258 w
$Fe(py)_4(NCS)_2$	2090 sh 2065 vs 2017 sh	810 m	483 m	271 s	199 s		965 w
$Fe(py)_4(NCSe)_2$	2065 vs	655 m	432 s	260 s	205 s		864 w
$Fe(py)_2Cl_2$				183 s	240 s 220 s		
$Fe(py)_2Br_2$				193 s[b]	242 s 220 s		
$Fe(py)_2I_2$				190 s	235 s		
$Fe(py)_2(NCO)_2$	2195 vs	1324 w 1332 w	*c*	280 s	222 s		
$Fe(py)_2(NCS)_2$	2150 sh 2090 vs 2050 sh	783 w	473 m	261 s	208 s	185 s	945 w
$Fe(py)_2(NCSe)_2$	2100 vs 2060 sh	608 w	417 m	228 s	197 s	187 s	845 w

[a] All data at ambient temperature in wavenumbers (cm^{-1}). Abbreviations: s, strong, m, medium; w, weak; v, very; sh, shoulder. [b] Tentative assignments. [c] Probably coincident with a pyridine band at 618 cm^{-1}.

transition is observed at 5760 cm^{-1} accompanied by several higher energy bands which sharpen considerably on cooling to 23 K. On cooling, the high-energy side of the $10Dq$ band decreases in intensity as a result of the thermal depopulation of vibrational excited states. The assignments and calculated values given in Table VIII have been estimated from a Tanabe–Sugano diagram by using the value of $10Dq$ obtained from the spectrum and 800 cm^{-1} for B and $C = 4B$. The estimated values are in good agreement with the observed spectrum. More detailed calculations which use the matrix elements given by Griffith[88] and which take into account configuration interaction are currently underway.[89] Several related tetrahedral iron(II) iodide complexes with bulky tertiary amine and aromatic amine ligands yield ligand field parameters of the order of 500 cm^{-1}.[89] Apparently, the nonbulky pyridine ligand with its good σ-bonding characteristics is able to form a relatively short iron–nitrogen bond and hence produce a larger ligand field.

Infrared Spectral Results. The fundamental infrared bands in pyridine and each of the iron(II) complexes are presented in Table IX.[22] In some instances, the fundamental modes are split upon coordination and several values are given. Our pyridine spectrum is identical with that obtained by Corrsin et al.[90] The assignment of the normal vibrational modes (Table IX) is that of Kline and Turkevich[91] and includes the more recent assignment of overtones.[90,91] Approximate descriptions of each of the modes are also given. In general, each of these bands shift to slightly higher energy (ca. 2–10 cm^{-1}) upon coordination. However, certain of these bands have a large shift to higher energy in each compound as summarized in Figure 14. It is not possible to explain these shifts on the basis of electronic σ- and π-bonding changes upon coordination. As a result, we believe that the increase is a result of pyridine ring/pyridine ring steric interactions within the coordination sphere of the tetrakis complexes or between pyridine and the bridging ligand in the bis complexes. In view of the relatively strong pyridine–iron bond, each of the normal modes (except 11) will tend to move the pyridine toward the center of the complex. Hence, for instance, the 8a mode will decrease the H(1) to C(5) distance on adjacent molecules,[42] increase the steric interaction, and shift the mode to higher energy. Similar arguments can be used for the other positive shifts. A normal-coordinate analysis[93] of the spectral bands in $M(py)_4Cl_2$ complexes is currently in progress to verify these ideas. This analysis is also supported by the work of Gill et al.,[94] who found

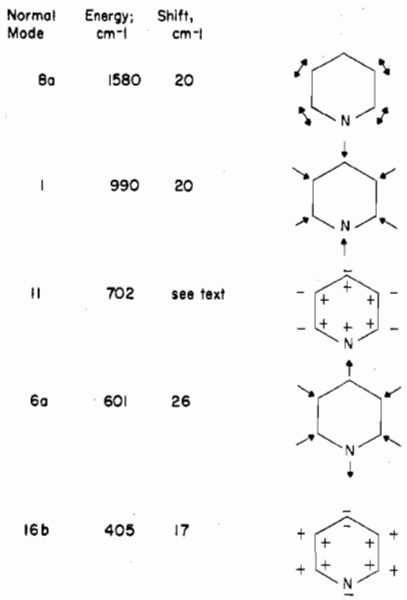

Figure 14. Selected normal vibrational modes for pyridine and their shift upon complexation.

that the 6a and 16b modes shifted to higher energy with decreasing central metal ionic radii. Only one line, 702 cm^{-1}, 11 mode, shifts on the average by 9 cm^{-1} to lower energy upon coordination—and then only in the bis(pyridine) compounds. Apparently this ring deformation is favored by both electronic and steric factors in the relatively more open bis complexes.

The low-frequency infrared spectrum of neat pyridine shows weak lines at 247 and 223 cm^{-1} and a moderately strong line at 168 cm^{-1}. No normal vibrational mode assignment has been made for these bands. The 168-cm^{-1} band is observed in several of the complexes. The weak bands at 247 and 223 cm^{-1} are obscured by strong metal–ligand bands in the complexes. The low-frequency infrared spectra of the halide complexes generally show two additional lines between 180 and 250 cm^{-1} which may be assigned to iron–ligand vibrational bands. Specific assignments are given in Table X and are in good agreement with work on related cobalt and nickel pyridine complexes.[95] The ν_{Fe-N} band is about 10–15 cm^{-1} higher in the bis(pyridine) compounds as might be expected because the pyridine molecules are more easily removed by thermolysis[40]

from the tetrakis than from the bis complexes. The same trend is observed in the bis- and tetrakis(pyridine)cobalt and -nickel chloride and bromide complexes.[95] As expected, the bridging iron–chloride band in $Fe(py)_2Cl_2$ is ca. 50 cm^{-1} lower than the terminal ν_{Fe-Cl} band in $Fe(py)_4Cl_2$. The ν_{Fe-I} band in $Fe(py)_4I_2$ and the ν_{Fe-Br} band in $Fe(py)_2Br_2$ seem rather high; hence, these assignments are tentative. The assignments for the $Fe(py)_2I_2$ support its pseudotetrahedral structure because its ν_{Fe-I} band would be expected to be higher than in the related octahedral compounds.[58,95]

The pseudohalide infrared bands are also presented in Table X. The positions of the thiocyanate and selenocyanate bands are indicative of terminal nitrogen bonding in the tetrakis complexes and bridging with both nitrogen and sulfur (or selenium) bonding in the bis complexes.[96] For instance, the ν_{NC-S} band at 810 cm^{-1} and the δ_{NCS} band at 481 cm^{-1} in $Fe(py)_4(NCS)_2$ are exactly the values expected for nitrogen-bonded thiocyanate[97,98] and are much too high for sulfur bonding.[96] The bridging thiocyanate shows each of these bands at values intermediate between the nitrogen and sulfur terminal bonded cases but resembling more closely the nitrogen-bonded case. This resemblance can be understood on the basis of the slightly smaller carbon–sulfur bond order in the bridging ligand as compared with the terminal nitrogen-bonded thiocyanate. The difference in the carbon–sulfur bond order is, of course, larger for the two terminal-bonded ligands.[99] Exactly the same arguments can be made for the bonds in the two selenocyanate complexes.[100] As pointed out by Bailey et al.,[101] the first overtone of the δ_{NCX} band is unusually intense especially for the nitrogen-bonded ligands. In most instances, we observe this first overtone and have included it in Table X.

The energy of the iron–pyridine vibrational bands reported in Table X for the pseudohalide complexes is surprisingly constant at ca. 200 cm^{-1} and is lower than in the halide complexes. The one exception is the $Fe(py)_2(NCO)_2$ where apparently the reduced pyridine interaction with the coordination sphere permits a shorter stronger bond. This bond is apparently weakest when the selenium atom in the NCSe group is bonded to the iron. The exact reason for the stronger iron–pyridine bonding in the halide complexes is not clear. The iron-to-nitrogen bond with the pseudohalide is typically stronger in the tetrakis complexes than in the bis complexes. This result is certainly consistent with our discussion above of the C–N and C–S bond order in the two types of pseudohalide coordination.[96] In the bridging thio- and selenocyanate complexes, an additional absorption at ca. 185 cm^{-1} is assigned to the ν_{Fe-XCN} band. These bands are at the lower end of the range expected for monodentate sulfur and selenium-bonded pseudohalides.[98,102] All of the assignments are in good agreement with related assignments for similar compounds.[95]

The infrared spectra of the cyanate complexes deserve particular attention because of the bidentate nitrogen bridging proposed in the $Fe(py)_2(NCO)_2$ complex. Unfortunately, the ν_{C-NO} and δ_{NCO} bands provide little basis for structural assignment in this complex. However, we would expect the ν_{NC-O} band to shift to lower energy if the oxygen were coordinated in the bridging ligand. Actually, this band is at essentially the same energy in both the bis and tetrakis complexes. This similarity supports the terminal nitrogen bridging ligand. A similar assignment for ν_{NCO} has been made by Nelson and Nelson,[103] who have assigned the terminal nitrogen bridge bonding structure to several cyanate complexes with substituted pyridine ligands. The frequency of the ν_{N-CO} band in these complexes is somewhat higher than we observe in $Fe(py)_2(NCO)_2$. However, a relatively low value for this band is probably reasonable in view of the three-center mode of nitrogen bonding. In addition, we observe no band between 300 and 500 cm^{-1} which could be assigned to the ν_{Fe-OCN} band. The failure of the cyanate ion to utilize its oxygen atom in bridge bonding has been explained on the basis of the charge distribution within the ion. The calculations of Wagner[104] indicate that the oxygen atom in the cyanate ion has a smaller negative charge on the oxygen than does the sulfur and selenium in thiocyanate and selenocyanate.

Acknowledgment. B.F.L. thanks the National Science Foundation for a Faculty Science Fellowship. G.J.L. thanks the United Kingdom Atomic Energy Research Authority for a Vacation Research Associate appointment in the Nuclear Physics Division of the AERE Harwell. The authors thank Drs. B. W. Dale, J. R. Ferraro, S. Foner, H. P. Leighly, G. Longworth, and W. M. Reiff for their many helpful discussions and Ms. M. Biolsi for the DTGA. The financial assistance of the National Science Foundation through Grants GP-8653 and CHE 75-20417 is gratefully appreciated.

Registry No. $Fe(py)_4Cl_2$, 15245-99-5; $Fe(py)_4Br_2$, 34406-12-7; $Fe(py)_4I_2$, 33572-47-3; $Fe(py)_4(NCO)_2$, 27489-00-5; $Fe(py)_4(NCS)_2$, 15225-68-0; $Fe(py)_4(NCSe)_2$, 24835-36-7; $Fe(py)_2Cl_2$, 27835-83-2; $Fe(py)_2Br_2$, 67688-52-2; $Fe(py)_2I_2$, 67688-60-2; $Fe(py)_2(NCO)_2$, 67688-54-4; $Fe(py)_2(NCS)_2$, 27835-85-4; $Fe(py)_2(NCSe)_2$, 67688-56-6; $Co(py)_4Cl_2$, 14077-25-9; $Ni(py)_4Cl_2$, 36829-43-3; $Co(py)_4Br_2$, 14129-02-3; $Ni(py)_4Br_2$, 14129-05-6; $Co(py)_4I_2$, 67814-26-0; $Ni(py)_4I_2$, 14077-31-7; $Co(py)_4(NCO)_2$, 67737-45-5; $Co(py)_4(NCS)_2$, 15727-35-2; $Co(py)_4(NCSe)_2$, 67737-46-6; $Co(py)_2Cl_2$, 29469-41-8; $Ni(py)_2Cl_2$, 26602-22-2; $Co(py)_2Br_2$, 14024-83-0; $Ni(py)_2Br_2$, 26602-23-3; $Co(py)_2I_2$, 14025-00-4; $Ni(py)_2I_2$, 14025-04-8; $Co(py)_2(NCO)_2$, 15627-26-6; $Co(py)_2(NCS)_2$, 26297-43-8; $Co(py)_2(NCSe)_2$, 67688-58-8.

Supplementary Material Available: Tables I (elemental analyses), II (X-ray powder diffraction *d* spacings), III (magnetic susceptibilities), and IX (fundamental IR bands) and Figures 5 (Mössbauer spectrum of $Fe(py)_4(NCS)_2$), 6 (Mössbauer spectra for transformation of pure $Fe(py)_4(NCSe)_2$ to pure $Fe(py)_2(NCSe)_2$), 10 (electronic spectra of $Fe(py)_2(NCS)_2$, $Fe(py)_2(NCSe)_2$, and $Fe(py)_4(NCSe)_2$), and 11 (electronic spectra of $Fe(py)_2Br_2$, $Fe(py)_4Br_2$, and $Fe(py)_4I_2$) (13 pages). Ordering information is given on any current masthead page.

References and Notes

(1) G. J. Long, D. L. Whitney, and J. E. Kennedy, *Inorg. Chem.*, **10**, 1406 (1971).
(2) W. M. Reiff, R. B. Frankel, B. F. Little, and G. J. Long, *Inorg. Chem.*, **13**, 2153 (1974).
(3) S. Foner, R. B. Frankel, W. M. Reiff, B. F. Little, and G. J. Long, *Solid State Commun.*, **16**, 159 (1975).
(4) S. Foner, R. B. Frankel, E. J. McNiff, Jr., W. M. Reiff, B. F. Little, and G. J. Long, *AIP Conf. Proc.*, No. **24**, 363 (1975).
(5) W. M. Reiff, R. B. Frankel, B. F. Little, and G. J. Long, *Chem. Phys. Lett.*, **28**, 68 (1974).
(6) R. M. Golding, K. F. Mok, and J. F. Duncan, *Inorg. Chem.*, **5**, 774 (1966).
(7) J. F. Duncan, R. M. Golding, and K. F Mok, *J. Inorg. Nucl. Chem.*, **28**, 1114 (1966).
(8) C. D. Burbridge, D. M. L. Goodgame, and M. Goodgame, *J. Chem. Soc. A*, 349 (1967).
(9) J. P. Sanchez, L. Asch, and J. M. Friedt, *Chem. Phys. Lett.*, **18**, 250 (1973).
(10) H. Sano and M. Kanno, *Chem. Lett.*, 127 (1973).
(11) M. Takeda, T. Tominaga, and N. Saito, *J. Inorg. Nucl. Chem.*, **36**, 2459 (1974).
(12) P. B. Merrithew, J. J. Guerrera, and A. J. Modestino, *Inorg. Chem.*, **13**, 644 (1974).
(13) P. B. Merrithew, P. G. Rasmussen, and D. H. Vincent, *Inorg. Chem.*, **10**, 1401 (1971).
(14) T. Tominaga, T. Morimoto, M. Takeda, and N. Saito, *Inorg. Nucl. Chem. Lett.*, **2**, 193 (1966).
(15) T. Tominaga, M. Takeda, T. Morimoto, and N. Saito, *Bull. Chem. Soc. Jpn.*, **43**, 1093 (1970).
(16) G. J. Long and W. A. Baker, *J. Chem. Soc. A*, 2956 (1971).
(17) M. Gerloch, R. F. McMeeking, and A. M. White, *J. Chem. Soc., Dalton Trans.*, 2452 (1975).
(18) H. T. Witteveen, W. L. C. Rutten, and J. Reedijk, *J. Inorg. Nucl. Chem.*, **37**, 913 (1975).
(19) M. Goldstein and W. D. Unsworth, *Spectrochim. Acta, Part A*, **28**, 1107 1297 (1972); *Inorg. Chim. Acta*, **4**, 342 (1970).
(20) D. M. L. Goodgame, M. Goodgame, M. A. Hitchman, and M. J. Weeks, *Inorg. Chem.*, **5**, 635 (1966).
(21) C. D. Burbridge and D. M. L. Goodgame, *Inorg. Chim. Acta*, **4**, 231 (1970).

(22) Supplementary material.
(23) G. Spacu and V. Armeanu, *Bull. Soc. Stiinte Cluj*, **7**, 566 (1934).
(24) B. F. Little, Doctoral Dissertation, University of Missouri-Rolla, 1979; B. F. Little and G. J. Long, *Appl. Spectrosc.*, in preparation.
(25) C. D. Burbridge, M. J. Cleare, and D. M. L. Goodgame, *J. Chem. Soc. A*, 1698 (1966).
(26) "Gmelins Handbuch der Anorganischen Chemie", Vol. 58, Verlag Chemie, GMBH, Weinheim, 1963, p 71.
(27) N. S. Gill, R. S. Nyholm, G. A. Barclay, T. I. Christie, and P. J. Pauling, *J. Inorg. Nucl. Chem.*, **18**, 88 (1961).
(28) J. R. Allan, D. H. Brown, R. H. Nuttall, and D. W. A. Sharp, *J. Inorg. Nucl. Chem.*, **26**, 1895 (1964).
(29) S. M. Nelson, *Proc. Chem. Soc., London*, 372 (1961).
(30) A. Hantzsch, *Z. Anorg. Allg. Chem.*, **159**, 273 (1927).
(31) F. A. Cotton, D. M. L. Goodgame, M. Goodgame, and T. E. Haas, *Inorg. Chem.*, **1**, 565 (1962).
(32) S. M. Nelson and T. M. Shepherd, *J. Chem. Soc.*, 3276 (1965).
(33) D. J. Hamm, J. Bordner, and A. F. Schreiner, *Inorg. Chim. Acta*, **7**, 637 (1973).
(34) M. D. Glonek, C. Curran, and J. V. Quagliano, *J. Am. Chem. Soc.*, **84**, 2014 (1962).
(35) W. J. Potts, Jr., "Chemical Infrared Spectroscopy", Vol. I, Wiley, New York, 1963.
(36) G. J. Long, Doctoral Dissertation, Syracuse University, 1968.
(37) B. N. Figgis and R. S. Nyholm, *J. Chem. Soc.*, 4190 (1958).
(38) J. R. DeVoe, Ed., *Natl. Bur. Stand. (U.S.) Tech. Note*, **No. 404**, 108 (1966).
(39) G. Lang and B. W. Dale, *Nucl. Instrum. Methods*, **116**, 567 (1974).
(40) B. F. Little and G. J. Long, *Inorg. Chim. Acta*, submitted for publication.
(41) K. Burger, G. Liptay, L. Korecz, I. Kiraly, and E. Papp-Molnar, "Proceedings of the Third Symposium on Coordination Chemistry", Debrecen, Hungary, 1970, M. T. Beck, Ed., Publishing House of the Hungarian Academy of Sciences, Budapest, 1971, p 465.
(42) G. J. Long and P. J. Clarke, *Inorg. Chem.*, **17**, 1394 (1978).
(43) M. A. Porai-Koshits and A. S. Antsyshkina, *Tr. Inst. Kristallogr., Akad. Nauk. SSSR*, **10**, 117 (1954).
(44) I. Søtofte and S. E. Rasmussen, *Acta Chem. Scand.*, **21**, 2028 (1967).
(45) M. A. Porai-Koshits and A. S. Antsyshkina, *Sov. Phys.—Crystallogr. (Engl. Transl.)*, **3**, 694 (1958).
(46) J. D. Dunitz, *Acta Crystallogr.*, **10**, 307 (1957).
(47) P. J. Clarke and H. J. Milledge, *Acta Crystallogr., Sect. B*, **31**, 1543, 1554 (1975).
(48) K. N. Baranski, L. A. Gribov, and V. P. Prikhod'ko, *Sov. Phys.—Crystallogr. (Engl. Transl.)*, **1**, 280 (1956).
(49) M. A. Porai-Koshits and G. N. Tischchenko, *Kristallografiya*, **4**, 239 (1959); *Sov. Phys.—Crystallogr. (Engl. Transl.)*, **4**, 216 (1960).
(50) D. A. Rowley and R. S. Drago, *Inorg. Chem.*, **6**, 1092 (1967).
(51) M. Gerloch, R. F. McMeeking, and A. M. White, *J. Chem. Soc., Dalton Trans.*, 655 (1976).
(52) S. Akyuz, A. B. Dempster, J. E. D. Davies, and K. T. Holmes, *J. Chem. Soc., Dalton Trans.*, 1746 (1976).
(53) R. M. Barr, M. Goldstein, and W. D. Unsworth, *J. Crystallogr. Mol. Structure*, **4**, 165 (1974).
(54) N. S. Gill, R. H. Nuttall, D. E. Scaife, and D. W. Sharp, *J. Inorg. Nucl. Chem.*, **18**, 79 (1961).
(55) D. M. L. Goodgame, M. Goodgame, and M. J. Weeks, *J. Chem. Soc.*, 5194 (1964).
(56) B. N. Figgis, J. Lewis, F. E. Mabbs, and G. A. Webb, *J. Chem. Soc. A*, 442 (1967).
(57) B. N. Figgis, "Introduction to Ligand Fields", Interscience, New York, 1966, p 265.
(58) R. C. Dickinson and G. J. Long, *Inorg. Chem.*, **13**, 262 (1974).
(59) G. J. Long and D. L. Coffen, *Inorg. Chem.*, **13**, 270 (1974).
(60) J. T. Wrobleski and G. J. Long, *Inorg. Chim. Acta*, **30**, 221 (1978).
(61) T. Birchall and M. F. Morris, *Can. J. Chem.*, **50**, 211 (1972).
(62) D. Forster and D. M. L. Goodgame, *J. Chem. Soc.*, 454 (1965).
(63) F. Petillon, J. E. Guerchais, and D. M. L. Goodgame, *J. Chem. Soc., Dalton Trans.*, 1209 (1973).
(64) R. Ingalls, *Phys. Rev.*, **155**, 157 (1967).
(65) N. N. Greenwood and T. C. Gibb, "Mössbauer Spectroscopy", Chapman and Hall, London, 1971, p 50.
(66) A value above 0.78 indicates that the crystallographic *c* axis is not always exactly normal to the γ-ray. A single-crystal study of isomorphic $Co(py)_4Cl_2$ doped with ^{57}Fe gave a ratio of 0.78.
(67) R. L. Collins and J. C. Travis, "Mössbauer Effect Methodology", Vol. 3, I. J. Gruverman, Ed., Plenum Press, New York, 1967, p 123.
(68) G. J. Long and B. W. Dale, unpublished results.
(69) A. S. Artsyshkina and M. A. Porai-Koshits, *Sov. Phys. Crystallogr. (Engl. Transl.)*, **3**, 684 (1959).
(70) W. M. Reiff, G. J. Long, and B. F. Little, *Inorg. Nucl. Chem. Lett.*, **12**, 405 (1976).
(71) R. Ingalls, *Phys. Rev.* [*Sect.*] *A*, **133**, A787 (1964).
(72) D. S. McClure, "Advances in the Chemistry of Coordination Compounds", S. Kirschner, Ed., Macmillan, New York, 1961, p 498.
(73) K. F. Purcell and J. C. Kotz, "Inorganic Chemistry", W. B. Saunders, Philadelphia, 1977, p 545.
(74) T. C. Gibb, *J. Chem. Soc. A*, 1439 (1968).
(75) M. Gerloch and R. F. McMeeking, *J. Chem. Soc., Dalton Trans.*, 2443 (1975).
(76) C. K. Jørgensen, "Modern Aspects of Ligand Field Theory", North-Holland Publishing Co., Amsterdam, 1971, p 176.
(77) A. H. Norbury, P. E. Shaw, and A. I. P. Sinha, *J. Chem. Soc., Dalton Trans.*, 742 (1975).
(78) W. L. Steffen and G. J. Palenik, *Inorg. Chem.*, **16**, 1119 (1977).
(79) B. R. Hollebone, *J. Chem. Soc. A*, 481 (1971).
(80) F. W. Klaaijsen, Z. Dokoupil, and W. J. Huiskamp, *Physica*, **79B**, 547 (1975).
(81) C. E. Johnson in "Hyperfine Structure and Nuclear Radiations", E. Matthias and D. A. Shirley, Eds., North-Holland Publishing Co., Amsterdam, 1968, p 226.
(82) J. Chappert, *Rev. Phys. Appl.*, **12**, 71 (1974).
(83) G. J. Long, W. M. Reiff, and B. F. Little, unpublished results.
(84) P. R. Edwards, C. E. Johnson, and R. J. P. Williams, *Chem. Phys.*, **47**, 2074 (1967).
(85) D. P. Shoemaker and C. W. Garland, "Experiments in Physical Chemistry", 2nd ed., McGraw-Hill, New York, 1967, p 34.
(86) C. E. Schaffer, *Struct. Bonding (Berlin)*, **14**, 69 (1973).
(87) M. Gerloch and R. C. Slade, "Ligand-Field Parameters", Cambridge University Press, London, 1973, p 185.
(88) J. S. Griffith, "The Theory of Transition Metal Ions", Cambridge University Press, London, 1964, p 412.
(89) G. J. Long and V. T. Wilcox, unpublished results.
(90) L. Corrsin, B. J. Fax, and R. C. Lord, *J. Chem. Phys.*, **21**, 1170 (1953).
(91) C. H. Kline and J. Turkevich, *J. Chem. Phys.*, **12**, 300 (1944).
(92) G. Zerbi, B. Crawford, and J. Overend, *J. Chem. Phys.*, **38**, 127 (1963).
(93) G. J. Long and B. F. Little, unpublished results.
(94) N. S. Gill, R. H. Nuttall, D. E. Scaife, and D. W. A. Sharp, *J. Inorg. Nucl. Chem.*, **18**, 79 (1961).
(95) J. R. Ferraro, "Low-Frequency Vibrations of Inorganic and Coordination Compounds", Plenum Press, New York, 1971.
(96) R. A. Bailey, S. L. Kozak, T. W. Michelsen, and W. N. Mills, *Coord. Chem. Rev.*, **6**, 407 (1971).
(97) J. Lewis, R. S. Nyholm, and P. W. Smith, *J. Chem. Soc.*, 4590 (1961).
(98) A. Sabatini and I. Bertini, *Inorg. Chem.*, **4**, 959 (1965).
(99) C. W. Frank and L. R. Rogers, *Inorg. Chem.*, **5**, 615 (1966).
(100) Reference 96, p 424.
(101) Reference 96, p 412.
(102) Reference 95, p 249.
(103) J. Nelson and S. M. Nelson, *J. Chem. Soc. A*, 1597 (1969).
(104) E. L. Wagner, *J. Chem. Phys.*, **43**, 2728 (1965).